

Thermal Infrared Image Analysis for Breast Cancer Detection

Sedong Min¹, Jiyoung Heo², Youngsun Kong³, Yunyoung Nam^{3,*}, Preap Ley⁴, Bong-Keun Jung⁵, Dongik Oh¹, Wonhan Shin⁶

¹Medical Information Communication Technology, Soonchunhyang University, Asan, Republic of Korea
[e-mail: sedongmin@sch.ac.kr, dohhea@gmail.com]

²Department of ICT Convergence Rehabilitation Engineering, Soonchunhyang University, Asan, Republic of Korea
[e-mail: wldud8965@hanmail.net]

³Department of Computer Science and Engineering, Soonchunhyang University, Asan, Republic of Korea
[e-mail: vengeful224@gmail.com, ynam@sch.ac.kr]

⁴Sihanouk Hospital Center of HOPE, Cambodia
[e-mail: preapley@yahoo.com]

⁵Department of Occupational Therapy, College of Medical Science, Soonchunhyang University, Republic of Korea
[e-mail: jungb@sch.ac.kr]

⁶Department of Neurosurgery, Soonchunhyang University Hospital, Bucheon, Republic of Korea
[e-mail: shinwh@schmc.ac.kr]

*Corresponding author: Yunyoung Nam

*Received September 6, 2016; revised November 14, 2016; accepted December 3, 2016;
published February 28, 2017*

Abstract

With the rise in popularity of photographic and video cameras, an increasing number of fields are now using thermal imaging cameras. One such application is in the diagnosis of breast cancer, as thermal imaging provides a low-cost and noninvasive method. Thermal imaging is particularly safe for pregnant women, and those with large, dense, or sensitive breasts. In addition, excessive doses of radiation, which may be used in traditional methods of breast cancer detection, can increase the risk of cancer. This paper presents one method of breast cancer detection. Breast images were taken using a thermal camera, with preliminary experiments conducted on Cambodian women. Then the experimental results were analyzed and compared using Shannon entropy and logistic regression.

Keywords: breast cancer, thermal camera, neural network, relative entropy

A preliminary version of this paper was presented at APIC-IST 2016, and was selected as an outstanding paper. This work was supported by the Soonchunhyang University Research Fund and also supported by the Bio & Medical Technology Development Program of the NRF funded by the Korean government, MSIP(NRF-2015M3A9D7067219).

1. Introduction

Breast cancer is one of the more prolific types of cancer, with a high incidence and mortality rate [1] [2], accounting for approximately 25% of cancers in women worldwide [3]. According to 2012 data from the United Kingdom, for stage 1 through stage 3 breast cancer, the 1-year survival rate is more than 97%, and for stage 4, the rate is 71% [4]. Moreover, patients' 5-year survival rate plummets from 99% in those detected with stage 1 cancer to 15% in those detected with stage 4 cancer [4].

The variation in prognosis and survival rates of breast cancer patients is highly dependent upon early detection of this disease [5, 6]. Various diagnosis methods have been developed to detect breast cancer in the early stages. For example, the breast self-examination method requires participants to check for lumps in the breasts by palpating the breast tissue. It is not only a low-cost method, but also no risk of excessive radiation exposure; however, the accuracy is typically lower than that of other methods, which can lead to increased healthcare costs [5, 7]. Screening for breast cancer using mammography, which magnifies particular parts of the breasts using low-energy X-rays, is another diagnostic method that decreases mortality rates and allows diagnosis of early stage breast cancer. While the compression can cause discomfort or pressure, it should be painful for most women [6]. Ultrasonography is relatively inexpensive and does not expose participants to ionizing radiation; however, it typically does not effectively detect calcifications [8]. Magnetic resonance imaging (MRI) can also be used to detect breast cancer tumors, but the overall costs are considerably high for both the equipment and maintenance [9]. Therefore, new methods are required to safely diagnose breast cancer at a low cost.

Recently, there has been considerable interest in small low-cost thermal cameras, particularly because they can be utilized for medical research with the development of more advanced sensor technology and image processing techniques [10]. Moreover, current advances in smartphone technology allows users to easily obtain thermal images, and advances in thermal cameras present the possibility of breast cancer diagnosis using mobile devices [11]. Furthermore, pregnant women can be diagnosed without exposure to radiation. However, due to the complexity of thermal breast cancer images, it is difficult to analyze and diagnose these images reliably.

Numerous studies [12–15] using thermal images for breast cancer detection have verified the feasibility of this technique. In [12] and [13], thermal images were analyzed with statistical features, and were classified using the support vector machine (SVM) and fuzzy algorithms, respectively. In [14], wavelet transformation was used to decompose thermal images to detect tumors. From this, principal component analysis (PCA) was used to compact the features. Finally, an artificial neural network (ANN) was used to classify normal and abnormal images. The authors used high-resolution thermal images and achieved an accuracy of 90.48%, but image data were not classified with clinical decision. In [15], breast regions were obtained from thermal images using the Hough transform algorithm, after which histogram and co-occurrence features were extracted to analyze the distribution of images. The authors used ANN to classify normal and abnormal images with an accuracy rate of 96.12%. However, these methods have not been verified against clinical data; therefore, they can only be used as diagnostic aids to help clinicians. In addition, more expensive cameras are needed to provide high-resolution images.

In this paper, the red, green and blue (RGB) histograms and co-occurrence feature vectors were estimated from thermal images using ANN. In addition, this method was compared between the left and right breast, using discrete wavelet transform (DWT) with Shannon entropy. The remainder of the paper is organized as follows. In Section 2, the preprocessing of thermal images is described, in which breast regions were extracted while eliminating the background. Section 3 describes the methods of histogram analysis, and its features, as well as a co-occurrence matrix, entropies with wavelet transform, and RGB channels. In Section 4, experiments are presented. Finally, Section 5 discusses and concludes the paper.

2. Preprocessing of thermal images

Fig. 1 shows thermal images obtained from FLIR A320 [16] and iPhone FLIR One [17] using different resolutions. In general, thermal images obtained from healthy subjects had a uniform distribution of heat, whereas those obtained from unhealthy patients had a relatively uneven distribution [18].

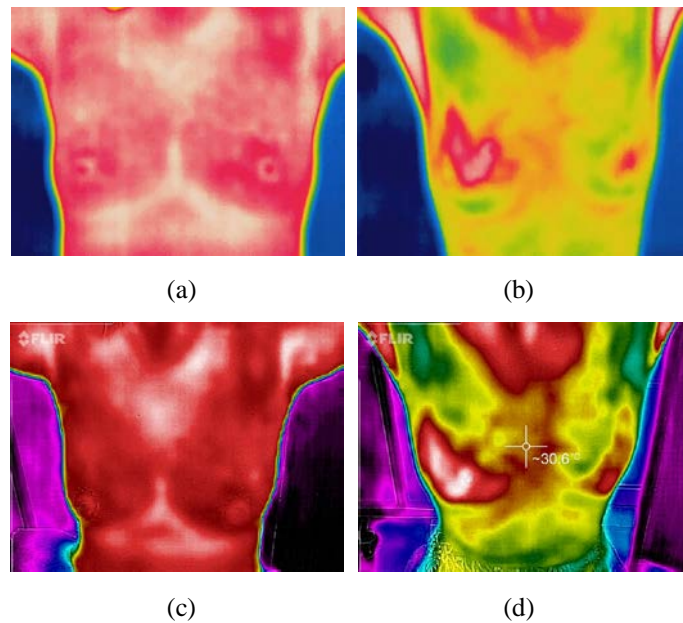


Fig. 1. Thermal images obtained from (a) (b) FLIR A320 and (c) (d) FLIR One. (a) a healthy, (b) a patient, (c) a healthy, (d) a patient

2.1 Background Elimination

The typical background temperature greatly differs from that of the human body. Therefore, the background in thermal images should be removed to focus on the regions of interest (ROI). **Fig. 2** shows a flow chart of the background elimination method. First, the red channel was extracted from the images. Then, Gaussian filter was used to draw edges from images using a Canny edge detector. Finally, the Hough transform was used to reinforce this calculated edge. **Fig. 3** shows each RGB channel of a thermal image. The red channel was selected to eliminate the background as it provided the best results of Canny edge algorithm among all of the channels. **Fig. 4** shows a comparison of detected contours when the Gaussian filter was both

applied and not applied. Finally, Fig. 5 shows a final foreground image after eliminating background.

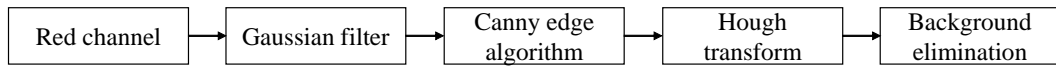


Fig. 2. Flow chart of background elimination

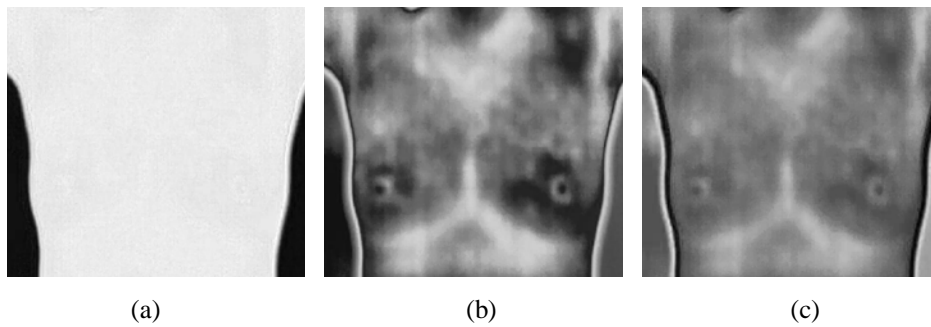


Fig. 3. RGB channels of a thermal image. (a) red channel, (b) green channel, (c) blue channel

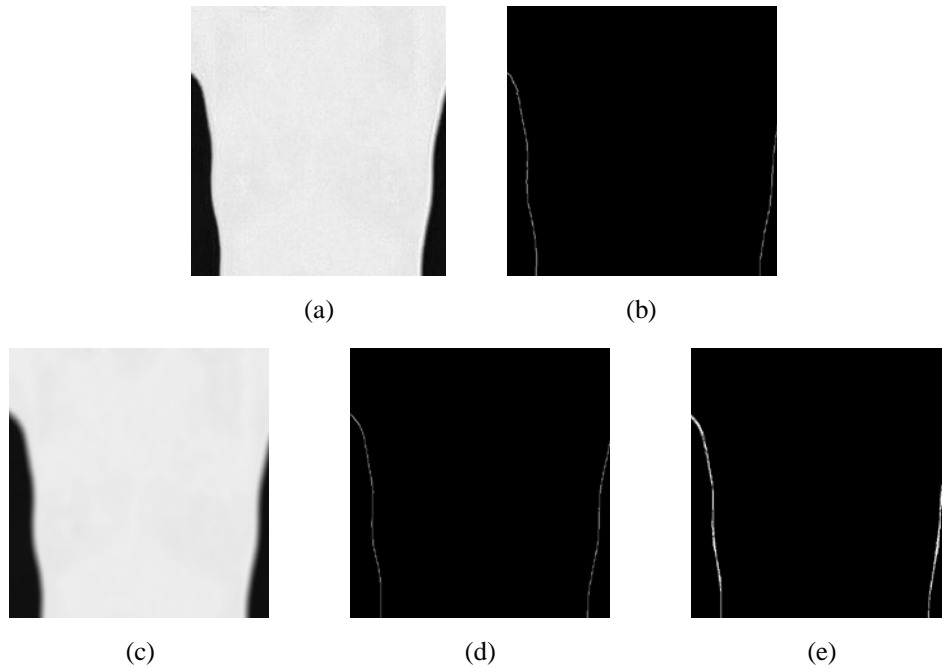


Fig. 4. Contour detection from red channel using a Gaussian filter, a Canny edge algorithm and Hough transform. (a) red channel where the Gaussian filter was not applied, (b) detected contour, (c) red channel where the Gaussian filter was applied; (d) detected contour, (e) strengthened contour

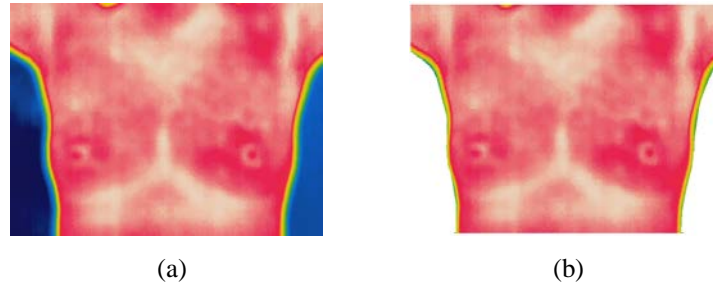


Fig. 5. Foreground images after eliminating background.
(a) an original image; (b) a foreground image

2.2 Region of Interest Identification

Fig. 6 shows a flow chart of auto ROI detection. Images were separated into three bands (red, green, and blue) and transformed into gray scale. Then, auto ROI detection was conducted and estimated four times by each channel.

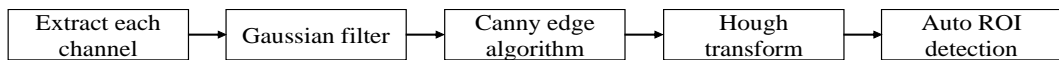


Fig. 6. Flow chart of ROI detection

After a single channel was extracted, the edge was drawn using the Gaussian filter and the canny edge algorithm. Finally, two circles were extracted using the Hough transform. **Fig. 7** shows an example of the difference between a Gaussian filter and no filter applied. With no filter applied, ROIs were extracted at the wrong position, while ROIs were extracted at the correct position using a Gaussian filter. Two parameters were set to improve the ROI detection rate: the radius for the Hough transform and the distance between the circles. The radius for the Hough transform parameters were set by the Euclidian distance, ranging from 100 to 200 pixels in a thermal image. In addition, the minimum Euclidian distance between the left and right centroid circles was set to 50 pixels.

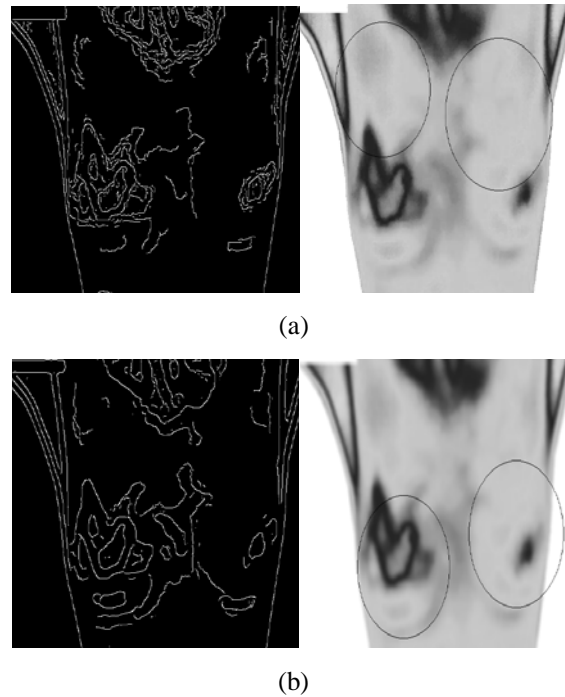


Fig. 7. Comparison when a Gaussian filter is not applied (a) and is applied (b)

3. Feature extraction and analysis

Fig. 8 shows histograms of a healthy subject and a patient. The histogram shows the frequency of pixels in the ROI (i.e., the probability distribution function in the intensity of the images). Twelve color features were used for classification including mean, variance, skewness, and kurtosis of each RGB channel. However, breasts that are not cancerous could have a higher temperature in certain areas (e.g., because of menstrual period or other diseases). **Fig. 9** shows the vertical co-occurrence matrixes of thermal images from a healthy subject and a patient. Both distributions of the co-occurrence matrix had a linear shape, and minute fluctuation among pixels could be estimated from the co-occurrence matrices. Twenty features, including energy, entropy, contrast, homogeneity and correlation of horizontal, vertical, diagonal, and anti-diagonal directions from gray channel, were used for classification.

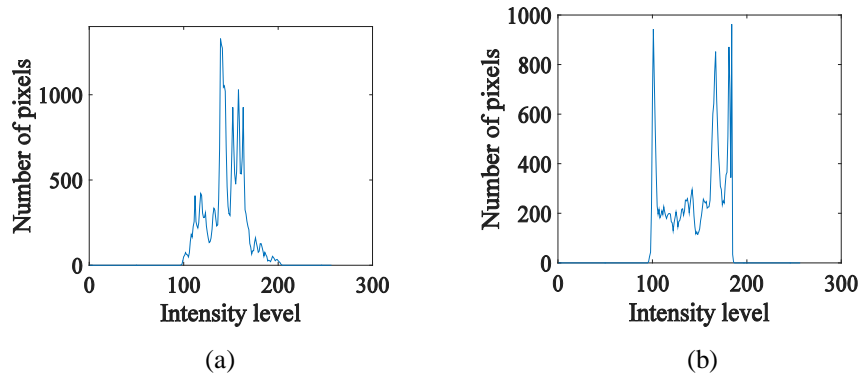


Fig. 8. Comparison of histogram between healthy subject and a patient.
(a) healthy subject; (b) patient

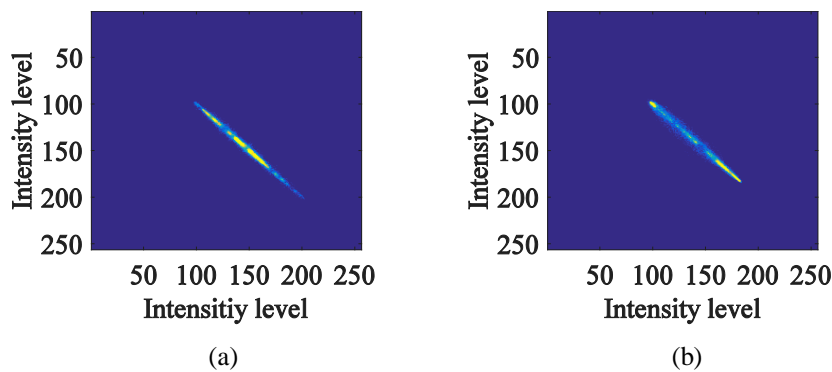


Fig. 9. Comparison of vertical co-occurrence matrixes between a healthy subject and a patient.
(a) a healthy subject; (b) a patient

3.1 Wavelet Transform

Color-based features (RGB channels) cannot be exploited to analyze spatial and frequency characteristics. Thus, Wavelet Transforms have been used to analyze both the spatial and frequency domain of one-dimensional signal and two-dimensional images [19]. In this paper, a DWT was applied when extracting features from breast images. Four sub-bands were obtained from one level of DWT. The Low-Low (LL) sub-band was a coarse approximation of the source image, and Low-High (LH), High-Low (HL), and High-High (HH) sub-bands were detail coefficients that included horizontal, vertical, and diagonal details, respectively. LH, HL, and HH sub-bands of breast images were obtained as features, and their Shannon entropies were calculated. **Fig. 10** shows the decomposed sub-bands of the breast cancer image.

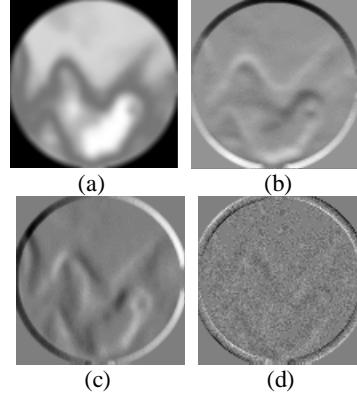


Fig. 10. Decomposition of a breast cancer image. (a) LL, (b) LH, (c) HL, (d) HH

3.2 Shannon Entropy

To compare uncertainties between left and right breasts, dominant features should be chosen. Shannon entropy [20] was used to analyze the complexity of an image. In this paper, Shannon entropy was used as a feature to compare the left and right breasts. Shannon entropy was estimated as follows:

$$Entropy = - \sum p \log_2 \frac{p}{q}, \quad (10)$$

where p and q represent the distribution of pixels and maximum entropy, respectively. Shannon entropies were obtained from RGB and gray channels, and of HL, LH, and HH bands decomposed by DWT.

Table 1 shows the experimental results of entropies estimated by the green and gray channels of images obtained from two healthy subjects and one patient. In the case of the patient, the difference in the green channel was 0.23, which was larger than that of the gray channel (0.12). Thus, the green channel was determined to be the most suitable channel among the RGB and gray channels.

Table 1. Results of estimating entropy from green and gray channels

Subject	Entropy				Note
	Green channel		Gray channel		
	Left	Right	Left	Right	
Patient	0.85	0.62	0.86	0.74	Right breast cancer
Healthy subject 1	0.8	0.8	0.8	0.78	
Healthy subject 2	0.83	0.82	0.81	0.82	

Table 2 shows the experimental results of entropies calculated by HL, LH, HH bands decomposed using DWT obtained images from two healthy subjects and one patient. All of the wavelet bands were used as a classification feature due to the non-existence of a dominant sub-band.

Table 2. Results of estimating entropy from wavelet bands

Subject	Entropy						Note
	HL		LH		HH		
	Left	Right	Left	Right	Left	Right	
Patient	0.31	0.52	0.32	0.56	0.32	0.42	Right breast cancer
Healthy subject 1	0.51	0.49	0.52	0.47	0.39	0.41	
Healthy subject 2	0.44	0.41	0.36	0.46	0.56	0.38	

4. Experimental Results

4.1 Experiments

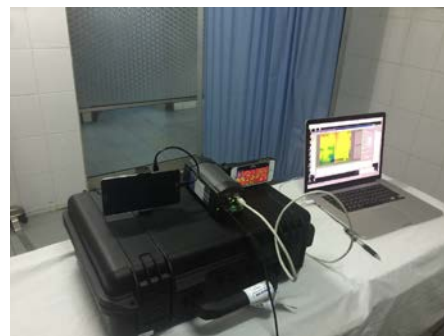
In this paper, 250 thermal images were collected from one female patient and 125 healthy subjects with ages ranging from 16 to 67. As shown in **Fig. 11**, the thermal images were captured at 320×240 (FLIR A320) and 80×60 (FLIR One) pixel resolutions. All subjects were instructed to capture images twice with arms raised and lowered. Matlab and OpenCV Library were used for analyzing these data.



(a)



(b)



(c)

Fig. 11. Experimental setup. (a) overall, (b) front, (c) back

4.2 Results

Table 3 shows the ROI detection rate estimated from red, green, blue and gray channels of images captured by FLIR A320 and FLIR One. The ROI detection result of the green channel was the highest rate at 84.55% (FLIR A320) and 77.6% (FLIR One). Therefore, the green channel was used to extract further ROI.

Table 3. ROI detection rate from red, green, blue and gray channels

Device	ROI detection Rate (%)			
	Red channel	Green channel	Blue channel	Gray channel
FLIR A320	56.09	84.55	79.67	77.23
FLIR One	65.6	77.6	68	65.6

Table 4 shows the ROI detection rate estimated from images that are applied a Gaussian filter. The result shows that the accuracy of filtered images was larger than that of the non filtered images. Thus, the Gaussian filter was applied to the images for ROI detection..

Table 4. ROI detection rate from images applied a Gaussian filter

Device	ROI detection Rate (%)	
	No filter	Gaussian filter
FLIR A320	77.24	84.55
FLIR One	71.2	77.6

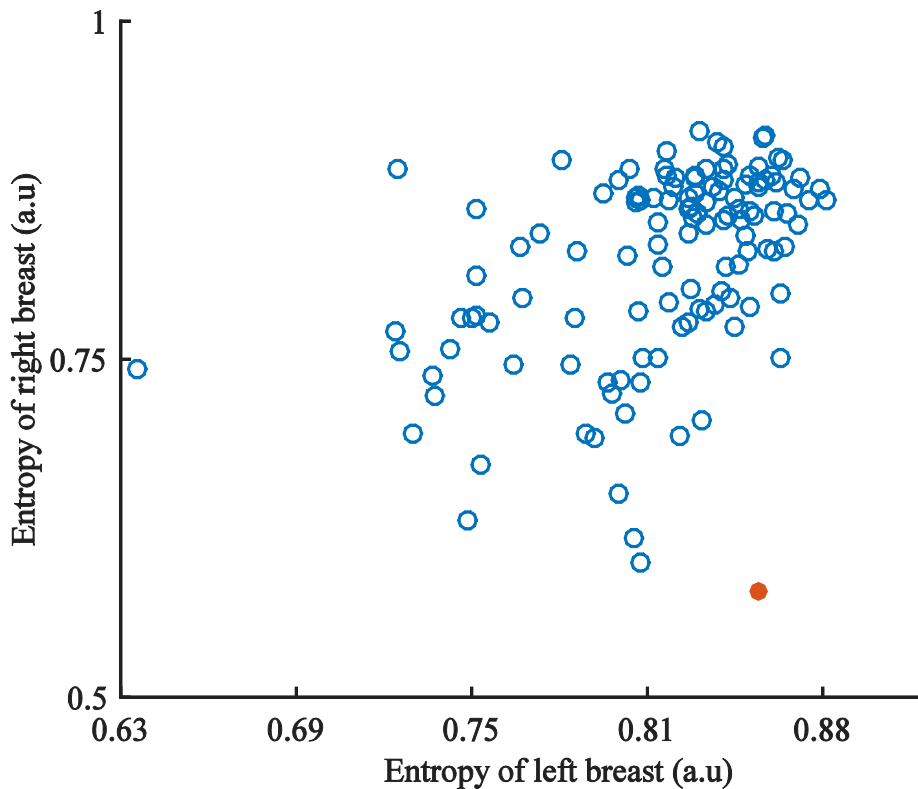


Fig. 12. Entropy distribution from a green channel

Fig. 12 shows the distribution of entropies estimated by the green channel. The red dot and empty dot represent entropies of a patient and healthy subjects, respectively. Entropies of the left and right breasts of a patient, who had breast cancer in the right breast, were 0.85 and 0.62, respectively. A proportion of the entropies were 0.73, while an average proportion of entropies of healthy subjects was 0.96. A patient who has breast cancer can be separated from others as shown in **Fig. 12**.

Fig. 13 shows the distribution of entropies in the left and right breast, as estimated with DWT. The black diamond and empty diamond represent the entropy proportions of a patient and healthy subjects, respectively. Red and yellow diamonds represent a breast cancer patient whose arm was raised and dropped, respectively. Entropy proportions between the left and right breasts of two images of a patient who had breast cancer in the right breast were 1.26, 1.28, 1.08 and 1.67, 1.73, 1.31, respectively (LH, HL, HH). The result show that breast cancer cannot be diagnosed using only Shannon Entropy with DWT. However, subjects who have breast cancer can be separated from healthy subjects due to with different entropies from those of healthy subjects.

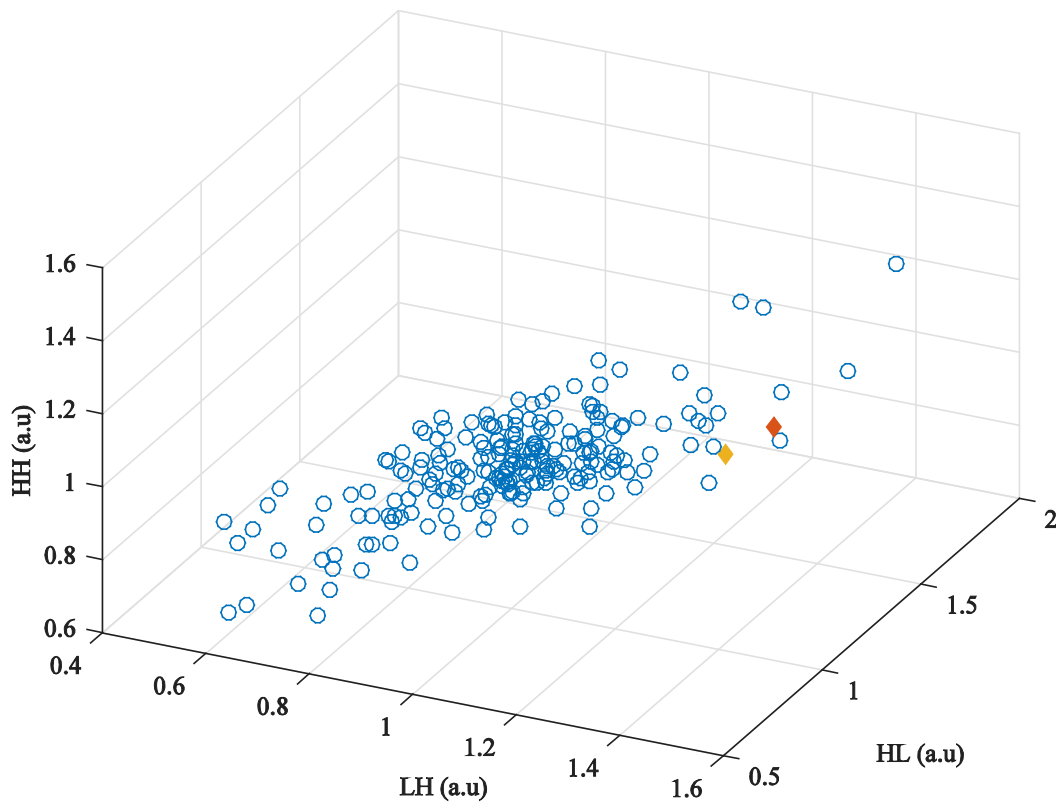


Fig. 13. Distribution of entropies proportion of wavelet bands.

Table 5 shows the experimental results of logistic regression using vector features obtained in section 3.2.2. 217 images were used for classification with a ten-fold cross validation. The sensitivity and specificity values were 98.6% and 50%, respectively.

Table 5. Confusion matrix for logistic regression

		Weka Results	
		Patient	Healthy subject
Clinical Decision	Patient	1	1
	Healthy subject	3	212

5. Discussions

This paper have presented a method of breast cancer diagnosis, based on several methods using thermal images. It used extracted ROIs after background extraction, which was then compared to various features estimated from the left and right breasts using Shannon entropy. Although the number of subjects in this experiment was low, to allow for precise diagnosis and to select individual features, a larger number of subjects in future work will make it possible to show improved accuracy from learning algorithms. A number of misdiagnosed images occurred due to other factors, such as the subjects' menstrual period and other diseases, which result in additional heat. Some features showed similar results to breast cancer. In the future, this method will be improved to achieve a high accuracy rate using low-resolution thermal images.

References

- [1] Porter, Peggy L., "Global trends in breast cancer incidence and mortality," *salud pública de méxico* 51, s141-s146, 2009.
- [2] Ahmedin, Elizabeth Ward, and Michael J. Thun, "Recent trends in breast cancer incidence rates by age and tumor characteristics among US women," *Breast Cancer Research* 9.3 R28, 2007.
- [3] World Cancer Report 2014. World Health Organization. 2014. pp. Chapter 1.1. ISBN 92-832-0429-8.
- [4] Cancer Research UK (2016), Breast cancer survival statistics, Cancer Research UK.
- [5] Lauver, D., "Addressing infrequent cancer screening among women," *Nursing outlook* 40.5, 207-212, 1991.
- [6] Tabár, László, and Peter B. Dean, "Breast Cancer-The Art and Science of Early Detection with Mammography," 2005.
- [7] Kusters JP, Gotzsche PC., Regular self-examination or clinical examination for early detection of breast cancer. *Cochrane Database Syst Rev.*, (2): CD003373, 2003. [Article \(CrossRef Link\)](#).
- [8] Nothacker, Monika, et al., "Early detection of breast cancer: benefits and risks of supplemental breast ultrasound in asymptomatic women with mammographically dense breast tissue. A systematic review," *BMC cancer* 9.1, 335, 2009.
- [9] Lehman, Constance D., et al., "MRI evaluation of the contralateral breast in women with recently diagnosed breast cancer," *New England Journal of Medicine* 356.13, 1295-1303, 2007. [Article \(CrossRef Link\)](#).
- [10] Diakides, Mary, Joseph D. Bronzino, and Donald R. Peterson, eds. *Medical Infrared Imaging: Principles and Practices*. CRC press, 2012.
- [11] Kapoor, Pragati, S. V. A. V. Prasad, and Ekta Bhayana, "Real time intelligent thermal analysis approach for early diagnosis of breast cancer," *International Journal of computer applications* 1.5 22-24, 2010.
- [12] Schaefer, Gerald, Michal Závisek, and Tomoharu Nakashima, "Thermography based breast cancer analysis using statistical features and fuzzy classification," *Pattern Recognition* 42.6, 1133-1137, 2009. [Article \(CrossRef Link\)](#).
- [13] Acharya, U. Rajendra, et al., "Thermography based breast cancer detection using texture features and support vector machine," *Journal of medical systems* 36.3, 1503-1510, 2012. [Article \(CrossRef Link\)](#).
- [14] Pramanik, Sourav, Debotosh Bhattacharjee, and Mita Nasipuri, "Wavelet based thermogram analysis for breast cancer detection," in *Proc. of Advanced Computing and Communication (ISACC), 2015 International Symposium on. IEEE*, 2015. [Article \(CrossRef Link\)](#).

- [15] Mohamed, Nader Abd El-Rahman, "Breast Cancer Risk Detection Using Digital Infrared Thermal Images," *American Institute of Science*, Vol. 1, No. 2, pp. 185-194, 2015.
- [16] FLIR A320 Datasheet, FLIR Systems, http://www.flir.com/uploadedFiles/Thermography_APA-C/Products/Product_Literture/090722%20A320%20datasheet_eng.pdf
- [17] FLIR ONE for iPhone 5/5s User manual, FLIR Systems, <http://www.flir.com/flirone/press/FLIR-ONE-User-Manual.pdf>
- [18] Sudharsan, N. M., E. Y. K. Ng, and S. L. The, "Surface temperature distribution of a breast with and without tumour," *Computer methods in biomechanics and biomedical engineering* 2.3, 187-199, 1999. [Article \(CrossRef Link\)](#).
- [19] Burrus, C. Sidney, Ramesh A. Gopinath, and Haitao Guo, "Introduction to wavelets and wavelet transforms: a primer," 1997.
- [20] C. E. Shannon, "A mathematical theory of communication," *Bell SystTech. J.*, vol. 27, p. 379-423/623-656, 1948.



Se Dong Min received the M.S. and Ph.D. degrees in electrical and electronic engineering from the Department of Electrical and Electronics Engineering, Yonsei University, Seoul, in 2004 and 2010, respectively. He is currently an Assistant Professor at the Department of Medical IT Engineering, Soonchunhyang University, Asan, Korea. His research area includes biomedical signal processing, healthcare sensor application, and mobile healthcare technologies.



Jiyoung Heo received the B.S. degree in computer science and engineering from Soonchunhyang University, Asan Korea in 2016. She is currently pursuing a master degree in the Department of ICT Convergence Rehabilitation Engineering at Soonchunhyang University. Her research interests include image processing, pattern recognition, wearable computing and biomedical signal processing.



Youngsun Kong received the B.S. degree in computer science and engineering from Soonchunhyang University, Korea in 2015. He is currently pursuing a master degree in the Department of Computer Science and Engineering at Soonchunhyang University. His research interests include image processing, pattern recognition, wearable computing and biomedical signal processing.



Yunyoung Nam received the B.S., M.S., and Ph.D. degrees in computer engineering from Ajou University, Korea in 2001, 2003, and 2007 respectively. He was a Senior Researcher in the Center of Excellence in Ubiquitous System (CUS) from 2007 to 2010. He was a Research Professor in Ajou University from 2010 to 2011. He also spent time as a Visiting Scholar at Center of Excellence for Wireless & Information Technology (CEWIT), Stony Brook University, New York. He was a Postdoctoral Fellow at Worcester Polytechnic Institute, Massachusetts from 2013 to 2014. He is currently an assistant professor in the Department of Computer Science and Engineering at Soonchunhyang University. His research interests include multimedia database, ubiquitous computing, image processing, pattern recognition, context-awareness, conflict resolution, wearable computing, intelligent video surveillance, cloud computing, and biomedical signal processing.



Preap Ley Cambodian General Surgeon who graduated from Medical National University of Mongolia since 2005. He graduated the Surgical Fellowship Exchange Program of Soon Chun Hyang University, Bucheon Hospital, Korea in 2008. He graduated the Diagnostic Endoscopy course (Gastro- colonoscopy and bronchoscopy) in 2009. He got scholarship of International Visitor Leadership Program/Breast Cancer Awareness and Outreach supported by US State Department, USA, in 2011. He also graduated Surgical and Medical Oncology training in TATA Memorial Hospital, Mumbai, India in 2012. He was graduated and qualified in a Master of general surgery in 2008. He was an Assistant Professor of Topographical and Operative Surgery in 2009. He is a Surgical Director of Surgical Department of Sihanouk Hospital Center of HOPE since 2013.



Bong-Keun Jung received doctoral degree in occupational therapy from Washington University in St. Louis, Missouri, the USA. He is a professor in the department of Occupational Therapy and a principal investigator at ICT Convergence Rehabilitation Engineering Research Center at Soonchunhyang University. His current research interests include rehabilitation engineering, driving rehabilitation, and disability policy.



Dongik Oh is currently a professor at the Medical IT Engineering, SoonChunHyang University, South Korea. He received his B.S. degree in Computer Science from The City University of New York (College of Staten Island), USA in 1985; M.S. degree in Computer Science from Florida State University, USA in 1989; and Ph.D. degree in Computer Science from Florida State University, USA in 1997. His current area of research includes embedded systems, ubiquitous computing, healthcare systems, and mobile programming.



Won-Han Shin is a professor at the Department of Neurosurgery, Soonchunhyang University Bucheon Hospital, Bucheon, Korea. He received his M.D. degree in medicine from Medical college, Pusan National University, Busan, Korea in 1977. And his Ph.D. degree in medicine from Medical college, Soonchunhyang University, Asan, Korea in 1991. His current research interests are Medical ICT convergence field.